Unified Differential Spatial Modulation

Naoki Ishikawa, *Student Member, IEEE*, and Shinya Sugiura, *Senior Member, IEEE*

***Abstract*—This letter proposes a unified differential spatial modulation (DSM) architecture, where a flexible rate-diversity tradeoff is achieved, while enabling a simple single-RF transmitter structure along with non-coherent detection that dispenses with channel estimation at the receiver. In our proposed scheme, by assigning a set of sparse complex-valued antenna-index matrices, only one transmit antenna element is activated during each symbol interval and then a phase-shift keying (PSK) symbol is transmitted from the activated antenna element. The explicit benefit of the proposed scheme's universal DSM framework is ability to strike a balance between previous DSM schemes, such as the symbol-based and the block-based DSM schemes. Moreover, to attain a useful attainable diversity gain, we further extend the proposed DSM scheme in a manner that permits flexible planning of the number of symbols employed per antenna-index block.**

***Index Terms*—Differential encoding, MIMO, non-coherent detection, rate-diversity tradeoff, space-shift keying, space-time shift keying, spatial modulation.**

I. Introduction

RECENTLY, the high-rate spatial modulation (SM) multiple-input multiple-output (MIMO) concept [1], [2] has been extensively studied owing to the availability of a simple single-RF transmitter structure. The SM transmitter is characterized by the two encoding principles, i.e., single-antenna activation and amplitude phase shift keying (APSK) modulation. Although the SM scheme's increased transmission rate is not as substantial as that achievable by use of the full-multiplexing MIMO scheme, which is represented by Bell lab's layered space-time (BLAST) transmissions [3], the SM scheme's high scalability in the number of transmit antenna elements (AEs) is especially beneficial for large-scale/massive MIMO systems [4]. On the other hand, similar to other classic coherently-detected MIMO schemes, the SM scheme typically suffers from the limitations imposed by pilot overhead and channel estimation errors. This unhelpful effect becomes further disadvantageous when the number of transmit AEs is significantly high.

To combat this limitation, several differentially-encoded SM (DSM) schemes have been developed [5]–[9], where non-coherent detection is available at the receiver, thus dispensing with the need for pilot-based channel estimation. In [5], the so-called differentially-encoded space-time shift keying (DSTSK) was proposed as the first DSM scheme, which is capable of exploiting both the space- and time-dimensions, while the original SM scheme only relies on the spatial dimension. Specifically, this scheme utilized the unitary differential encoding principle, where one out of multiple space-time dispersion matrices is activated and then the activated matrix was differentially encoded after multiplied by an APSK-modulated symbol. Although this original DSTSK scheme requires the employment of full RF chains, its single-RF counterpart was also presented in [6] by constraining the structure of space-time dispersion matrices to be diagonal. In [7], the diagonal constraint was relaxed to improve achievable performance levels while maintaining a single-RF transmitter structure. Note that, in the DSTSK scheme, each APSK symbol is multiplied by an activated space-time dispersion matrix, i.e., an antenna-index matrix, that spans multiple symbol durations. In contrast, the original SM scheme activates an antenna element at every single symbol interval. This implies that while the DSTSK scheme is capable of attaining the desired diversity gain unlike the SM scheme, its transmission rate decreases due to the expanded time dimension per differentially-encoded block. Hence, in this letter the DSTSK scheme is referred to as the *block-based DSM scheme*.

More recently, in contrast to this block-based DSM scheme, the *symbol-based DSM scheme* was developed as reported in [8]. In this scheme, a binary antenna-index matrix set that contains the space and time dimensions is employed, while a phase-shift keying (PSK) symbol is multiplied during each symbol interval in the same manner as the original SM scheme [10], [11]. Since the product of such a sparse binary antenna-index matrix and a PSK symbol has a unitary matrix structure, each transmission power of the differentially encoded SM symbol is maintained at a constant that is similar to the above-mentioned DSTSK scheme [5]–[7].

Against this background, the novel contributions of this letter are as follows. We are the first to propose a unified DSM architecture, where a flexible rate-diversity tradeoff is achieved while simultaneously enabling a single-RF transmitter and a non-coherent detection aided receiver. Additionally, the number of symbols employed per antenna-index block is designed in a flexible manner, to permit attainment of an arbitrary transmit diversity order. Our proposed DSM scheme subsumes the previous DSTSK scheme [5]–[7] as well as the symbol-based DSM scheme [8] in its special cases. In terms of significant merit, the proposed scheme outperforms the symbol-based DSM scheme [8] without imposing any sacrifice and/or additional costs.

II. System Model

A. Proposed DSM Scheme

Let us begin by considering a DSM transmitter, which is equipped with M transmit AEs and a receiver, supporting N receive AEs. Assume that Q complex-valued sparse antenna-index matrices $\mathbf{A}_q \in \mathbb{C}^{M\times M} (q = 1, \ldots, Q)$ are assigned at the

Manuscript received February 18, 2014; accepted March 24, 2014. Date of publication April 4, 2014; date of current version August 20, 2014. This work was supported in part by the Strategic Information and Communications R&D Promotion Programme (SCOPE) of the Ministry of Internal Affairs and Communications, Japan, which is gratefully acknowledged. The associate editor coordinating the review of this paper and approving it for publication was H. H. Nguyen.

The authors are with the Department of Computer and Information Sciences, Tokyo University of Agriculture and Technology, Koganei 184-8588, Japan (e-mail: sugiura@ieee.org).

Color versions of one or more of the figures in this paper are available online at http://ieeexplore.ieee.org.

Digital Object Identifier 10.1109/LWC.2014.2315635

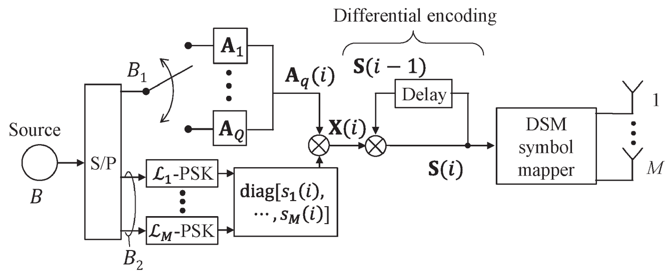

Fig. 1. The transmitter structure of our DSM system.

transmitter in advance of transmissions. Here, there is only a single non-zero component in each column of the Q matrices $\mathbf{A}_q (q = 1, \ldots, Q)$, which is represented by $a_{q,m}$ that satisfies the unit-norm relationship of $|a_{q,m}| = 1$ $(1 \leq q \leq Q, 1 \leq m \leq M)$. Additionally, M PSK modulation schemes are employed, where the associated constellation set is represented by $\mathbf{L} = [\mathcal{L}_1, \ldots, \mathcal{L}_M] \in \mathbb{Z}^M$.

The proposed differential block encoding procedure is given in Fig. 1. In each block interval, i.e., the M symbol durations, $B = \log_2(Q \cdot \mathcal{L}_1 \cdots \mathcal{L}_M)$ information bits are input to the proposed DSM modulation block. Then, B bits are serial-to-parallel (S/P) converted to $B_1 = \log_2 Q$ bits and $B_2 = \log_2(\mathcal{L}_1 \cdots \mathcal{L}_M)$ bits. Based on the B_1 bits, a single out of Q antenna-index matrix $\mathbf{A}_q(i)$ is activated, while the B_2 bits are mapped to M PSK symbols $\mathbf{s}(i) = [s_1(i), \ldots, s_M(i)]$. Here, i denotes the block index. Then, a matrix $\mathbf{X}(i) \in \mathbb{C}^{M \times M}$ is calculated as follows:

$$\mathbf{X}(i) = \text{diag}\left\{\mathbf{s}(i)\right\} \mathbf{A}_q(i) \tag{1}$$

where diag$\{\bullet\}$ represents the operation from a row vector to a diagonal matrix. Finally, a differentially-encoded space-time matrix $\mathbf{S}(i) \in \mathbb{C}^{M \times M}$ is calculated by

$$\mathbf{S}(i) = \mathbf{S}(i-1)\mathbf{X}(i) \tag{2}$$

which are transmitted from the M transmit AEs over M symbol durations. Note that the above-mentioned sparse constraint imposed on $\mathbf{A}_q(i)$, the unit-norm relationship $|a_{q,m}| = 1$ as well as the employment of the PSK symbol set enables us to maintain $\mathbf{X}(i)$ to be unitary, hence the norm of a space-time matrix $\mathbf{S}(i)$ becomes always constant.[1] Additionally, $\mathbf{S}(i)$ exhibits a sparse matrix structure, which contains only a single non-zero component in each column in the similar manner to antenna-index matrices $\mathbf{A}_q (q = 1, \ldots, Q)$. While the row vectors of $\mathbf{S}(i)$ correspond to the transmit AEs, each column is associated with a symbol index in the transmitted block. Hence, the number of activated transmit AEs during each symbol interval is always one, where the single-RF transmitter is satisfied. In this letter, we assumed that the first signal block of (2) is the identity matrix, i.e., $\mathbf{S}(0) = \mathbf{I}$, for simplicity.

[1]Unlike the previous scheme [12], our proposed DSM scheme is not capable of supporting quadrature amplitude modulation (QAM) symbols for $\mathbf{s}(i) = [s_1(i), \ldots, s_M(i)]$. More specifically, the proposed scheme utilizes multiple symbols per block, while [12] uses only a single symbol. Hence the normalization operation expressed by (41) of [12] is not directly applicable to our scheme.

To provide further insights, let us exemplify the proposed DSM transmitter having $(M = 3)$ transmit AEs and $Q = 4$ dispersion matrices of

$$\mathbf{A}_1 = \begin{bmatrix} a_{1,1} & 0 & 0 \\ 0 & a_{1,2} & 0 \\ 0 & 0 & a_{1,3} \end{bmatrix}, \ \mathbf{A}_2 = \begin{bmatrix} a_{2,1} & 0 & 0 \\ 0 & 0 & a_{2,3} \\ 0 & a_{2,2} & 0 \end{bmatrix}$$
$$\mathbf{A}_3 = \begin{bmatrix} 0 & a_{3,2} & 0 \\ a_{3,1} & 0 & 0 \\ 0 & 0 & a_{3,3} \end{bmatrix}, \ \mathbf{A}_4 = \begin{bmatrix} 0 & 0 & a_{4,3} \\ 0 & a_{4,2} & 0 \\ a_{4,1} & 0 & 0 \end{bmatrix} \tag{3}$$

where the coefficient $a_{q,m}$ represents the nonzero element in the mth column of the qth dispersion matrix.

The transmission rate of our DSM scheme is formulated by

$$R = \frac{B}{M} = \frac{\log_2(Q \cdot \mathcal{L}_1 \cdots \mathcal{L}_M)}{M} \tag{4}$$

which exhibits a higher transmission rate than that of the previous DSTSK scheme, which is represented by $\log_2(Q \cdot \mathcal{L})/M$. This is because our DSM scheme employs multiple PSK symbols per block, while only a single symbol is included per block in the DSTSK scheme.

At the receiver, the ith received signal block may be expressed as

$$\mathbf{Y}(i) = \mathbf{H}(i)\mathbf{S}(i) + \mathbf{V}(i) \tag{5}$$

where $\mathbf{H}(i) \in \mathbb{C}^{M \times M}$ are complex-valued channel coefficients and $\mathbf{V}(i) \in \mathbb{C}^{M \times M}$ are the corresponding additive white Gaussian noise (AWGN) components. Similarly, under the assumption that the channel coefficients remain unchanged over two successive blocks, specifically $\mathbf{H}(i) = \mathbf{H}(i-1)$, the $(i-1)$st received block is represented by

$$\mathbf{Y}(i-1) = \mathbf{H}(i)\mathbf{S}(i-1) + \mathbf{V}(i-1). \tag{6}$$

Then, based on (6), (5) is rewritten by $\mathbf{Y}(i) = \mathbf{H}(i)\mathbf{S}(i-1)\mathbf{X}(i) + \mathbf{V}(i) = \mathbf{Y}(i-1)\mathbf{X}(i) + \bar{\mathbf{V}}(i)$, where we have $\bar{\mathbf{V}}(i) = \mathbf{V}(i) - \mathbf{V}(i-1)\mathbf{X}(i)$. Finally, we arrive at the well-known maximum likelihood (ML) detection:

$$\begin{aligned} \hat{B} &= (\hat{q}, \hat{l}_1, \ldots, \hat{l}_M) \\ &= \arg \min_{(q, l_1, \ldots, l_M)} \\ &\quad \times \left\| \mathbf{Y}(i) - \mathbf{Y}(i-1)\text{diag}\left[\bar{s}_{l_1}, \ldots, \bar{s}_{l_M}\right] \mathbf{A}_q \right\|^2, \end{aligned}$$

where q is an activated antenna-index matrix. Furthermore, $0 \leq l_m \leq \mathcal{L}_M$ denotes the index of $\mathcal{L}_m$-size PSK constellation and $\bar{s}_{l_m}$ represents the associated PSK symbol.

B. Attaining Diversity Gain via Improved DSM Scheme

Similar to the symbol-based previous DSM scheme [8], the DSM scheme proposed in Section II-A is not capable of exploiting a useful diversity gain. This is because each PSK symbol is modulated per symbol interval, which makes it impossible to exploit any transmit diversity gain.Therefore, we will now extend the scheme of Section II-A to make it capable of attaining a diversity gain, while minimizing the decrease in a transmission rate. Note that it is a new idea to strike a rate-diversity tradeoff of the SM scheme by adjusting the number of different symbols in the diagonal matrix, rather than a space-time dispersion matrix structure itself. More specifically,

TABLE I
FUNDAMENTAL COMPARISONS BETWEEN THE PROPOSED AND PREVIOUS DSM SCHEMES

Type	Transmit diversity $\mathcal{D}$	block interval per symbol	Antenna-index matrices	Transmission rate R
Proposed DSM of Section II-A	$\mathcal{D} = 1$	One symbol	Complex-valued	$\log_2(Q \cdot \mathcal{L}_1 \cdots \mathcal{L}_M)/M$
Proposed DSM of Section II-B	$1 \leq \mathcal{D} \leq M$	$1 \leq \bar{M} \leq M$ symbols	Complex-valued	$\log_2(Q \cdot \mathcal{L}_1 \cdots \mathcal{L}_{\bar{M}})/M$
Block-based DSM (DSTSK) [6, 7, 9]	$1 \leq \mathcal{D} \leq M$	M symbols	Complex-valued	$\log_2(Q \cdot \mathcal{L})/M$
Symbol-based DSM [8]	$\mathcal{D} = 1$	One symbol	Binary	$\log_2(Q \cdot \mathcal{L}_1 \cdots \mathcal{L}_M)/M$

compared to the DSM of Section II-A, we reduce the number of PSK symbols per block from M to $\bar{M} < M$. For example, when we consider $M = 4$ transmit AEs, we may then have $(\bar{M} = 2)$ PSK symbols, which may be expressed as

$$\text{diag}\,[\mathbf{s}(i)] = \text{diag}\,[s_1(i), s_1(i), s_2(i), s_2(i)] \quad (7)$$

rather than diag$[s_1(i), s_2(i), s_3(i), s_4(i)]$ of Section II-A. The symbol allocation of (7) allows us to attain the transmit diversity order of $\mathcal{D} = 2$. In general, to have the transmit diversity order $\mathcal{D}$ in the proposed improved DSM scheme of this section, each PSK symbol has to span over at least $\mathcal{D}$ symbol durations, as shown in (7). Although this modification decreases the normalized transmission rate as follows: $R = B/M = \log_2(Q \cdot \mathcal{L}_1 \cdots \mathcal{L}_{\bar{M}})/M$, Here, the capability of attaining the transmit diversity gain enables us to benefit from the additional design degree-of-freedom.

In our proposed scheme, there are several design parameters, including (M, N, Q) and $(\mathcal{L}_1, \ldots, \mathcal{L}_{\bar{M}})$. More specifically, when BPSK and QPSK modulation schemes are employed for the above-mentioned model of (7), we use the following notation to represent a symbol set: $\mathbf{L} = [(\mathcal{L}_1, \mathcal{L}_1), (\mathcal{L}_2, \mathcal{L}_2)] = [(2, 2), (4, 4)]$.

III. SYSTEM DESIGN OF OUR DSM SCHEMES

A. Relationship With Previous DSM Schemes

As previously mentioned, the proposed DSM scheme employs a unified framework that subsumes the previous specific DSM schemes, such as the symbol-based [8] and the block-based DSM schemes [7]. For example, by limiting the nonzero components of our DSM scheme of Section II-A to be $a_{q,m} = 1$ $(1 \leq q \leq Q, 1 \leq m \leq M)$, our DSM scheme becomes equivalent to the symbol-based DSM scheme [8]. To be more specific, the $(M = 3)$ transmit-AE scenario, which is shown in Table I of [8], is represented by our proposed DSM scheme, having the following $(Q = 4)$ antenna-index matrices:

$$\mathbf{A}_1 = \begin{bmatrix} 1 & 0 & 0 \\ 0 & 1 & 0 \\ 0 & 0 & 1 \end{bmatrix}, \quad \mathbf{A}_2 = \begin{bmatrix} 1 & 0 & 0 \\ 0 & 0 & 1 \\ 0 & 1 & 0 \end{bmatrix},$$
$$\mathbf{A}_3 = \begin{bmatrix} 0 & 1 & 0 \\ 1 & 0 & 0 \\ 0 & 0 & 1 \end{bmatrix}, \quad \mathbf{A}_4 = \begin{bmatrix} 0 & 0 & 1 \\ 0 & 1 & 0 \\ 1 & 0 & 0 \end{bmatrix}. \quad (8)$$

Importantly, unlike the previous symbol-based DSM scheme [8], our DSM scheme is capable of supporting complex-valued elements $a_{q,m}$, rather than just binary elements, as in [8]. This enables our scheme to outperform that of [8] without imposing any additional costs. The detailed performance comparisons will be provided later in Section IV.

Similarly, the DSTSK scheme [7] is also expressed by our DSM scheme shown in Section II-B, which is capable of exploiting the transmit diversity gain. By simply constraining the number of different PSK symbols $\bar{M}$ in $\mathbf{s}(i)$ to $\bar{M} = 1$, the proposed DSM scheme becomes equivalent to the DSTSK scheme, which allows us to achieve the possible maximum attainable diversity order. To summarize the above-mentioned discussions regarding the DSM family, i.e., the two proposed DSM schemes of Sections II-A and II-B in addition to the previous symbol-based DSM scheme and the previous block-based DSM scheme, their fundamental characteristics are compared in Table I.

B. Antenna-Index Matrix Design

In the previous DSM scheme [8], which employs a binary antenna-index matrix set, the maximum number of antenna-index matrices Q is limited to $M! = M \cdot (M-1) \cdots 1$. By contrast, since the non-zero components of the matrices $\mathbf{A}_q (q = 1, \ldots, Q)$ are designed as complexed values in our DSM scheme, the maximum number of antenna-index matrices is not limited to $M!$. To fully exploit the potential high performance of our scheme, the antenna-index matrices have to be designed appropriately. The parameter design guideline of our DSM scheme shown in Section II-A is highlighted as follows:

- Given the number of transmit AEs M, the number of antenna-index matrices Q as well as a set of M PSK constellations $\mathbf{L} = [\mathcal{L}_1, \ldots, \mathcal{L}_M]$ are determined to attain a target transmission rate R according to (4).
- When we have the relationship of $M! > Q$, The $M \cdot Q$ non-zero positions of an antenna-index matrix set $\mathbf{A}_q (q = 1, \ldots, Q)$ are designed, in a way that ensures the minimum Hamming distance of any two antenna-index matrices is maximized by assuming $a_{q,m} = 1$. Otherwise, the non-zero positions and values are jointly designed with the aid of a specific metric and solution, as shown below.
- Finally, the $M \cdot Q$ non-zero components $a_{q,m}$, having the unit absolute values, are optimized, such that a desirable metric is maximized or minimized. To date, several design criteria have been proposed for the optimization of STSK and linear dispersion codes (LDCs) [2].

IV. PERFORMANCE RESULTS

In our simulations, we assumed the presence of quasi-static Rayleigh fading environments and primarily considered the two single-RF benchmark schemes, i.e., the symbol-based [8] and the block-based DSM schemes [6], [7], which are compared in Table I. The number of receive AEs was set to $N = 1$ for simplicity.

First, in Fig. 2 we compared our proposed DSM scheme and the symbol-based DSM scheme [8], while considering $M = 2$ transmit AEs. In Fig. 2(a) and (b) the transmission rates were $R = 1.5$ and 3.0 b/symbol, employing $\mathbf{L} = [2, 2]$ and [4,8] symbols, respectively. Additionally, we plotted the

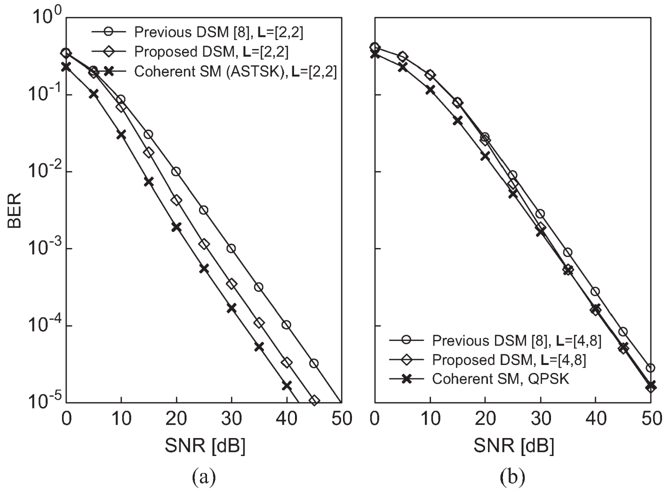

Fig. 2. The BER comparisons between our proposed DSM scheme and the symbol-based DSM scheme [8], while considering $M = 2$ transmit AEs. Also, we plotted the coherently-detected counterparts of the ASTSK [5] and the SM [10] schemes, respectively. (a) 1.5 b/symbol and (b) 3.0 b/symbol.

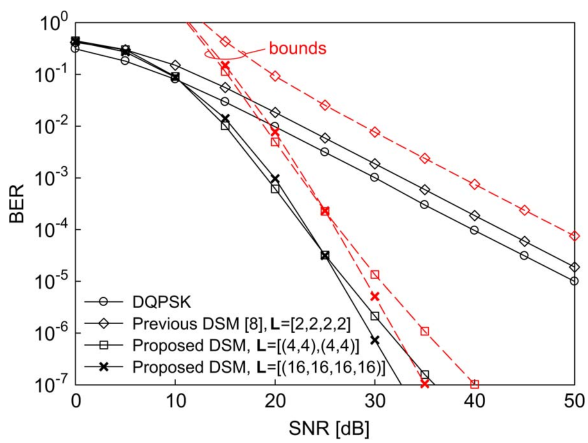

Fig. 3. The BER curves of our $(M, N, Q) = (4, 1, 16)$ DSM schemes proposed in Section II-B, having $\bar{M} = 2$ and 1 as well as those of the previous DSM scheme [8], employing four BPSK symbols, and of the single-antenna differential QPSK modulation were plotted as the benchmarks.

coherently-detected counterparts of the ASTSK [5] and the SM [10] schemes. Furthermore, the previous scheme has the $(Q = 2)$ binary antenna-index matrices, while the proposed scheme has the complex-valued ones. It should be noted that the non-zero positions and the number of antenna-index matrices were identical in all four DSM scenarios. Observe in Fig. 2 that our proposed scheme outperformed the DSM benchmark scheme without imposing any additional costs, and that neither schemes relied on a pilot overhead and/or channel estimation. However, note that upon increasing the constellation size, the performance advantages of our DSM scheme over the previous DSM scheme decreases, as predicted.[2]

An additional merit of our scheme is its capability of attaining a flexible transmit diversity gain. In Fig. 3 we plotted the two BER curves of our DSM schemes proposed in Section II-B, having $\bar{M} = 2$ and 1, respectively. The first curve corresponds to the $(Q = 16)$ antenna-index matrices and the $(\bar{M} = 2)$ QPSK symbols $\mathbf{L} = [(4, 4), (4, 4)]$, while the second one employs the same $(Q = 16)$ antenna-index matrices and $(\bar{M} = 1)$ 16-PSK symbol, i.e., $\mathbf{L} = [(16, 16, 16, 16)]$. Furthermore, the BER curves of the previous DSM scheme [8], employing four BPSK symbols, and of the single-antenna differential QPSK modulation were plotted as the benchmarks. Here, the transmission rate of all four DSM schemes was $R = 2.0$ b/symbols. Additionally, we plotted the loose theoretical error-rate bounds, which are derived according to [13]. In Fig. 3, it can be seen that both the proposed DSM schemes achieved the expected useful diversity gains, thus outperforming the two benchmark schemes.

V. Conclusion

This letter proposed the non-coherently detected DSM scheme, which dispenses with any channel estimation at the receiver, while benefiting from the SM scheme's fundamental advantages, such as the single-RF transmitter operation and the increased transmission rate. Furthermore, we extended the proposed DSM scheme to that capable of attaining a flexible transmit diversity gain.

[2]To investigate the impact of channels, we carried out additional simulations, where Rice fading as well as correlated Rayleigh fading was considered for the channel. As the results, it was found that our DSM scheme's advantage over the benchmark schemes remain unchanged.

References

[1] M. Di Renzo, H. Haas, A. Ghrayeb, S. Sugiura, and L. Hanzo, "Spatial modulation for generalized MIMO: Challenges, opportunities and implementation," *Proc. IEEE*, vol. 102, no. 1, pp. 56–103, Jan. 2014.

[2] S. Sugiura, S. Chen, and L. Hanzo, "A universal space-time architecture for multiple-antenna aided systems," *IEEE Commun. Surveys Tuts.*, vol. 14, no. 2, pp. 401–420, May 2012.

[3] P. Wolniansky, G. Foschini, G. Golden, and R. Valenzuela, "V-BLAST: An architecture for realizing very high data rates over the rich-scattering wireless channel," in *Proc. ISSSE*, 1998, pp. 295–300.

[4] J. Hoydis, S. ten Brink, and M. Debbah, "Massive MIMO in the UL/DL of cellular networks: How many antennas do we need?" *IEEE J. Sel. Areas Commun.*, vol. 31, no. 2, pp. 160–171, Feb. 2013.

[5] S. Sugiura, S. Chen, and L. Hanzo, "Coherent and differential space-time shift keying: A dispersion matrix approach," *IEEE Trans. Commun.*, vol. 58, no. 11, pp. 3219–3230, Nov. 2010.

[6] S. Sugiura, S. Chen, H. Haas, P. M. Grant, and L. Hanzo, "Coherent versus non-coherent decode-and-forward relaying aided cooperative space-time shift keying," *IEEE Trans. Commun.*, vol. 59, no. 6, pp. 1707–1719, Jun. 2011.

[7] S. Sugiura and L. Hanzo, "Effects of channel estimation on spatial modulation," *IEEE Signal Process. Lett.*, vol. 19, no. 12, pp. 805–808, Dec. 2012.

[8] Y. Bian, M. Wen, X. Cheng, H. V. Poor, and B. Jiao, "A differential scheme for spatial modulation," in *Proc. IEEE Global Commun. Conf.*, Atlanta, GA, USA, Dec. 9–13, 2013, pp. 4030–4035.

[9] S. Sugiura, "Coherent versus non-coherent reconfigurable antenna aided virtual MIMO systems," *IEEE Signal Process. Lett.*, vol. 21, no. 4, pp. 390–394, Apr. 2014.

[10] R. Y. Mesleh, H. Haas, S. Sinanovic, C. Ahn, and S. Yun, "Spatial modulation," *IEEE Trans. Veh. Technol.*, vol. 57, no. 4, pp. 2228–2242, Jul. 2008.

[11] M. Di Renzo and H. Haas, "Space shift keying (SSK) modulation with partial channel state information: Optimal detector and performance analysis over fading channels," *IEEE Trans. Commun.*, vol. 58, no. 11, pp. 3196–3210, Nov. 2010.

[12] S. Sugiura, C. Xu, S. X. Ng, and L. Hanzo, "Reduced-complexity coherent versus non-coherent QAM-aided space-time shift keying," *IEEE Trans. Commun.*, vol. 59, no. 11, pp. 3090–3101, Nov. 2011.

[13] M. R. Bhatnagar, A. Hjorungnes, and L. Song, "Differential coding for non-orthogonal space-time block codes with non-unitary constellations over arbitrarily correlated Rayleigh channels," *IEEE Trans. Wireless Commun.*, vol. 8, no. 8, pp. 3985–3995, 2009.